Polyimide Membranes: Ultra-Microporous Triptycene-based Polyimide Membranes for High-Performance Gas Separation (Adv. Mater. 22/2014)

ARTICLE *in* ADVANCED MATERIALS · JUNE 2014

Impact Factor: 17.49 · DOI: 10.1002/adma.201306229 · Source: PubMed

Ultra-Microporous Triptycene-based Polyimide Membranes for High-Performance Gas Separation

*Bader S. Ghanem, Raja Swaidan, Eric Litwiller, and Ingo Pinnau**

Triptycene-bearing polymers are widely versatile materials demonstrating high performance as potential low-K dielectrics and thin-film sensors with interlocked structures possessing unique combinations of modulus, strength and ductility.[1] These properties arise from the shape-persistent and three-dimensional structure of triptycene which traps "internal free volume" between three benzene arms bridged at 120° about a [2,2,2]-tricyclic ring system.[2] Triptycene's structure deems it an attractive candidate for a rigid contortion site in polymers of intrinsic microporosity (PIMs)[3] (pore dimension < 20 Å), in which inflexible kinked macromolecules can pack inefficiently to trap the microporosity characteristic of inorganic materials while preserving the organic tunability and solution-processability of amorphous polymers. PIMs have produced among the highest uptakes in gas storage applications[4] and advanced state-of-the-art materials in the rapidly growing field of industrial membrane-based gas separations.[5] With combinations of high gas permeabilities and low-to-moderate selectivities, PIMs overcome the Robeson trade-offs between gas permeability and selectivity, but more selective PIMs are required for commercial applications. The majority of PIMs to date, including prototypical PIM-1[6] and many of its derivatives, employ a flexible spiro center[7] for contortion. More rigid, bridged bicyclics have been shown to further improve permeability without significant changes in selectivity.[8]

Aromatic polyimides have broad commercial applications,[9] including membrane-based gas separations, because of their excellent thermal, physical and mechanical properties. PIM-polyimides (PIM-PIs) integrating a spiro center have been synthesized and demonstrated the highest gas permeabilities among polyimides, but their low selectivities still limit their performance to below the current 2008 upper bounds.[10,11] Despite the excellent gas sorption properties observed for insoluble triptycene-containing network PIMs,[12,13] only one report of gas separation properties for a solution-processable polyimide[14] exists. Known as 6FDA-DATRI, this thermally stable polyimide contains imide linkages to a flexible 2,6-diaminotriptycene, which results in significantly reduced microporosity (BET surface area, 68 m^2 g^{-1})[15] and, therefore, compromised permeability. Similar trends were observed in a recent report of an iptycene-containing polymer.[16] Moreover, early attempts to synthesize bridgehead-substituted triptycene polymers resulted in high crystallinity, brittleness, poor solubility and low molecular weight as well as poor gas separation properties.[17]

This Communication describes the synthesis and exceptional gas transport properties of two robust, solution-processable ultra-microporous (<7 Å) PIM-polyimides – KAUST-PI-1 and KAUST-PI-2 – integrating a three-dimensional 9,10-diisopropyltriptycene contortion center into a rigid fused-ring dianhydride. Rotation about the imide bonds is restricted by ortho-substituted methyl groups in the diamine. Bridgehead substitution at the 9,10-positions compounds the benefits of triptycene on three fronts:[13] First, it offers tunability of the porous texture; second, the triptycene imparts rigidity to short bridgehead substituents, effectively enhancing the overall three-dimensionality and rigidity of the moiety; third, it bolsters solution-processability by enhancing solubility. Functionalizing the bridgeheads with short branched isopropyl chains[18] primes the microstructure for highly permeable and highly selective diffusion-dominated performance surpassing all known polymers in industrial gas separations[5] including hydrogen (H_2/N_2, H_2/CH_4) and oxygen (O_2/N_2) separations, which constitute ~75% of the gas separation market.[19]

The synthesis of KAUST-PI-1 and KAUST-PI-2 is summarized in **Figure 1**a, beginning with the Diels-Alder addition of in-situ-formed benzyne to 9,10-diisopropyl-2,3,6,7-tetramethoxyanthracene to yield the 9,10-diisopropyl-2,3,6,7-tetramethoxytriptycene.[20] The dianhydride can be obtained by cyclodehydration of the corresponding tetracarboxylic acid produced by a short series of simple high-yield reactions: Demethylation of methoxy groups followed by aromatic nucleophilic substitution with 4,5-dichlorophthalonitrile, and alkaline hydrolysis thereof (Figure 1a).[10] The polymers were obtained in high molecular weight by high-temperature, one-step polymerization reactions between equimolar amounts of the dianhydride and commercially available diamines (2,3,5,6-tetramethyl-1,4-phenylene diamine, TMPD, and 3,3′,5,5′-tetramethylbenzidine, TMBZ) in *m*-cresol containing catalytic amounts of isoquinoline. The molecular structure of KAUST-PI-1 was confirmed by elemental analysis, ^{1}H-NMR, and FT-IR spectroscopy (Figure S1 and S2, Supporting Information (SI)). The disappearance of the absorption band at around 3400 cm^{-1} indicates full imidization of the polyamic acid. KAUST-PI-1 has no observable glass transition temperature and the triptycene moiety is thermally stable against retro-Diels Alder decomposition, showing no backbone degradation up to ~400 °C as typical of glassy and highly rigid polyimides (Figure S3, SI). It is readily soluble in many organic solvents and films were readily cast from chloroform (Table S1,

Dr. B. S. Ghanem, R. Swaidan, Dr. E. Litwiller, Prof. I. Pinnau
Advanced Membranes and Porous Materials Center
Physical Sciences and Engineering Division
King Abdullah University of Science and Technology (KAUST)
Al-Jazri Building, Thuwal 23955–6900, KSA
E-mail: Ingo.Pinnau@kaust.edu.sa

DOI: 10.1002/adma.201306229

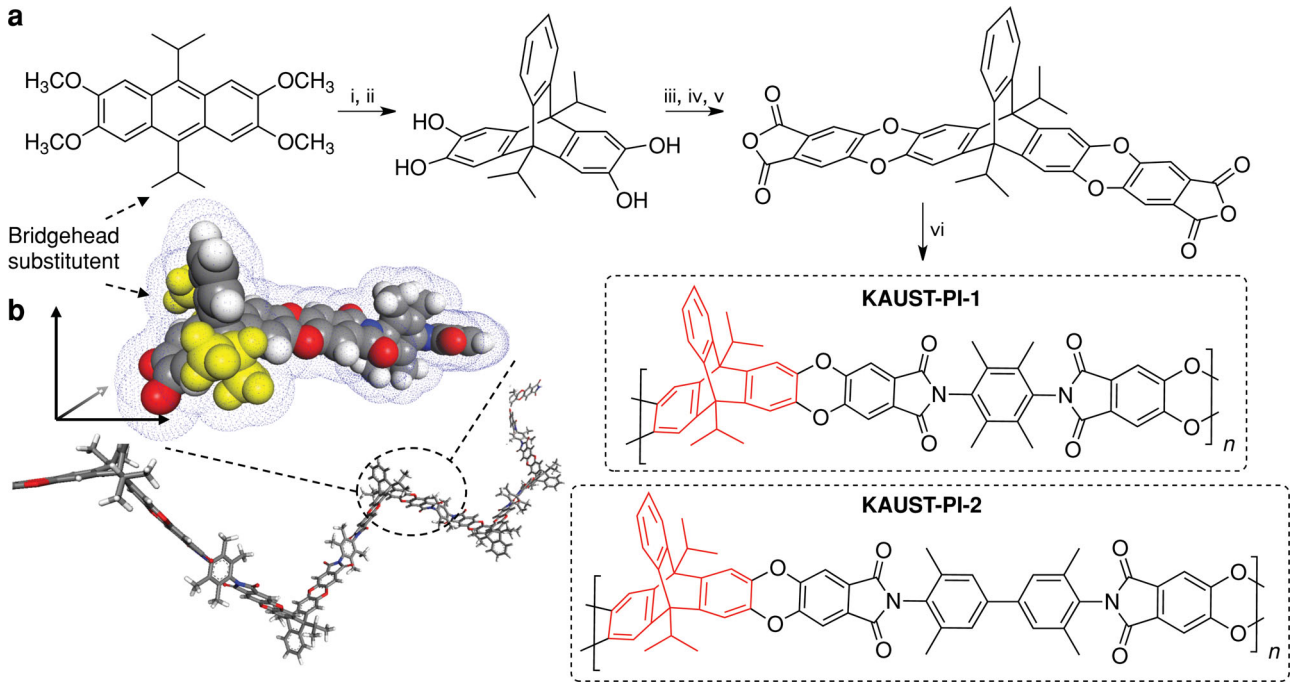

Figure 1. a) Synthesis of KAUST-PI-1. i. benzene diazonium chloride, $(CH_2)_2Cl_2$, 80 °C, 4 h; ii. BBr_3, CH_2Cl_2, 3 h; iii. 4,5-dichlorophthalonitrile, K_2CO_3, N,N-dimethylformamide (DMF), 80 °C, 10 h; iv. KOH, C_2H_5OH/H_2O, reflux 10 h; v. acetic anhydride, reflux 12 h; vi. diamine (TMPD or TMBZ), *m*-cresol, isoquinoline, 200 °C, 4 h. b) Geometrically optimized KAUST-PI-1 demonstrating contorted, ribbon-like growth and enhanced three-dimensionality afforded by the 9,10-diisopropyl-triptycene.

Figure S4 and S5, SI). Narrower energy wells detailed in the dihedral angle distributions (Figure S6, SI) indicate the greater intramolecular rigidity imparted by the triptycene moiety relative to the spiro center common to previous PIM-polyimides[10] and ladder PIMs like PIM-1 and PIM-SBF.[21] This was also observed for the bridged-bicyclic contortion centers in PIM-EA-TB.[8] Moreover, in stark contrast to the erratic chain growth spurred by the spiro center, an in-plane and ribbon-like chain growth appears in the geometrically optimized structure of triptycene-based KAUST-PI-1 (Figure 1b). Highlighted is a prominent three-dimensional character attributed to the lateral projection of isopropyl bridgehead-substituents and the transverse projections of the vertical aromatic ring and symmetric methyl groups in TMPD. Together, these key features serve as spacers that maintain inefficient packing of the ribbon-like chains and set the stage for ultra-microporosity. The synthesis and characterization of KAUST-PI-2 is similarly documented in the supporting information.

Isotropic membranes of KAUST-PI-1 and KAUST-PI-2 were cast from chloroform, soaked in methanol for 24 h and dried at 120 °C under vacuum for 24 hours for complete exchange of any residual casting solvent as confirmed by TGA (Figure S3, SI). It is known that relaxation of non-equilibrium free volume in highly microporous PIMs occurs rapidly in the first ~10 days after swelling in a non-solvent like methanol.[22] The gas permeation properties are strongly time-dependent in this region, as previously demonstrated for PIM-1 and shown here for KAUST-PI-1 (Figure S7, SI). For a more accurate representation of the gas separation potential of PIMs, gas transport properties should be determined in the quasi-steady-state period (10–12 days) showing stability on at least the experimental time scale. Accordingly, KAUST-PI-1 and KAUST-PI-2 exhibit extraordinary gas separation performance for a broad variety of high-impact applications in comparison to current PIM-polyimides, notable ladder-type PIMs including PIM-1, PIM-SBF and PIM-EA-TB (**Figure 2**). Both polymers transcend the latest polymer upper bounds for the O_2/N_2 gas pair, meeting the target for outcompeting rival technologies like cryogenic distillation in the challenging task of oxygen enrichment from air (Figure 2a).[23] Outstanding potential for efficient hydrogen (H_2/N_2, H_2/CH_4) recovery (Figure 2b and 2c) in ammonia purge-gas and petrochemical applications as well as the sweetening of natural gas via removal of CO_2 (Figure 2d) – among the fastest growing applications for membrane technology today – is also observed. KAUST-PI-1, in particular, bridges the gap between low free volume, highly selective commercial polymers and high free volume, highly permeable PIMs, permitting expansion of membrane applications into new high-capacity markets.

Interestingly, the permeability of H_2 (**Table 1**) for these polymers is greater than that of CO_2, opposite to what is conventionally observed for other spiro-based PIMs (PIM-1, PIM-PI-1, PIM-PI-9) where the high solubility of the larger CO_2 (k_D = 3.3 Å) affords it higher permeability than the smaller H_2 (k_D = 2.9 Å) (Table S2, SI). A similar ranking was reported for PIM-EA-TB and 6FDA-DATRI, which both contain bridged-bicyclics with roughly 120° kink angles. This is an indication that diffusivity selectivity, which capitalizes on minute differences in molecular size (e.g., 0.18 Å for O_2/N_2), dominates gas transport.

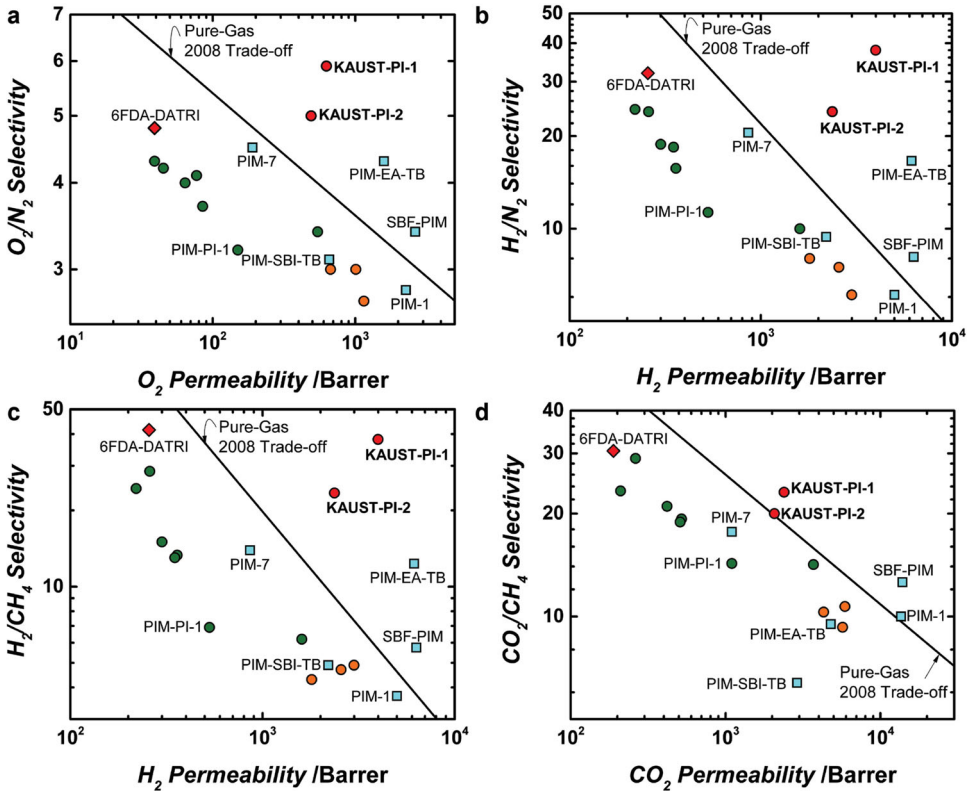

Figure 2. Separation performance for a) O_2/N_2 b) H_2/N_2 c) H_2/CH_4 d) CO_2/CH_4 gas pairs showing data for KAUST-PI-1 and KAUST-PI-2. Symbols represent notable materials from various classes including □ = Ladder PIMs,[6,8,21] ● = Extended[10] and ● = Non-extended[27] PIM-PIs. Solid lines represent state-of-the-art 2008 permeability/selectivity upper bounds.[5]

Table 1. Pure gas permeability, diffusivity and solubility coefficients for KAUST-PI-1 and KAUST-PI-2 at 35 °C and 2 bar. KAUST-PI-2 (57 μm). Data for KAUST-PI-1 is an average of measurements from two films (77 and 102 μm).

	Permeability	Diffusivity	Solubility
Gases	[10^{-10} cm^3(STP) cm cm^{-2} s^{-1} $cmHg^{-1}$]	[10^{-8} cm^2 s^{-1}]	[10^{-2} cm^3(STP) cm^{-3} $cmHg^{-1}$]
KAUST-PI-1			
He	1771	-[a)]	-[a)]
H_2	3983	-[a)]	-[a)]
N_2	107	31.2	3.43
O_2	627	158	3.98
CH_4	105	9.51	11.2
CO_2	2389	45.6	53.3
KAUST-PI-2			
He	1026	-[a)]	-[a)]
H_2	2368	-[a)]	-[a)]
N_2	98	28.9	3.39
O_2	490	138	3.56
CH_4	101	8.00	12.6
CO_2	2071	49.3	42.0

[a)]The time lag was too short for accurate calculations.

Typically, the solubility selectivity in polymers of a given class (e.g., hydrocarbon or perfluorocarbon) towards similarly sized penetrants is small and practically independent of chemical composition and microstructure.[24] For example, the O_2/N_2 solubility selectivity observed here is very similar to those measured for both low free-volume polymers and high free-volume PIMs (Table S3, SI). KAUST-PI-1 is an example of how integrating the 9,10-diisopropyl-triptycene into a rigid dianhydride with rigid imide linkages affords high diffusivity selectivities for molecular-sieving behavior (Table S2 and S3, SI). As the upper bounds illustrate (Figure 2), significant increases in gas selectivity (O_2/N_2, H_2/N_2, H_2/CH_4) over notable ladder-PIMs and PIM-PIs is achieved with comparatively high gas permeabilities. Even in KAUST-PI-2, where the TMBZ contributes extra flexibility to the backbone (Figure 1a), the effect of the diisopropyl-substituted triptycene on performance is dominant, maintaining combinations of permeability and selectivity beyond the polymeric upper bounds for various key applications.

The influence of the isopropyl-substituted triptycene moiety on gas transport properties is elucidated through qualitative studies of its impact on the polymeric microstructure,[25] here explored with physisorption isotherms (**Figure 3**a) and pore-size distribution (PSD) analyses (Figure 3b) obtained using N_2 at 77 K. KAUST-PI-1 has a BET surface area of 752 m^2 g^{-1}, the highest reported to date for a polyimide (i.e., 6FDA-DATRI,

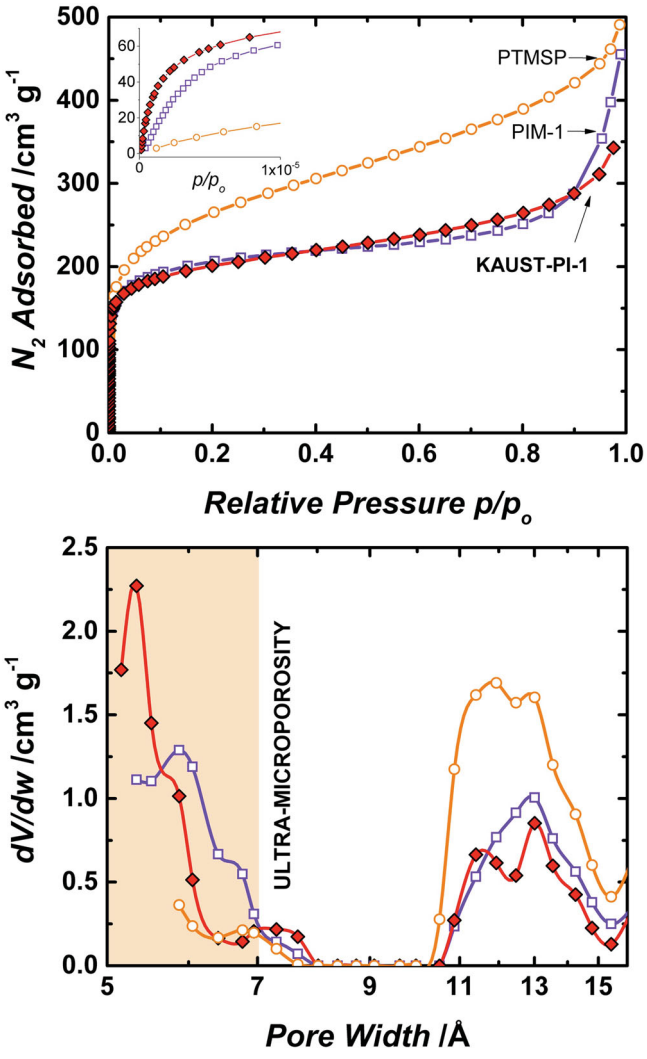

Figure 3. a) Nitrogen adsorption isotherms measured for PTMSP, PIM-1 and KAUST-PI-1 at 77 K. Saturation pressure, $p_o = 1$ bar. Inset zoomed to low-pressure region indicative of ultra-microporosity. b) NLDFT-analyzed pore-size distributions based on carbon slit-pore geometry, revealing shifts to ultra-microporosity in KAUST-PI-1.

68 m^2 g^{-1}; PIM-PI-1, 682 m^2 g^{-1}; PIM-PI-9, 690 m^2 g^{-1}). It displays high gas uptakes almost identical to those of ladder-type PIM-1 (768 m^2 g^{-1}), indicating the presence of a highly interconnected microporous structure. As the PSDs indicate (Figure 3b), the porous textures of these PIMs comprise a bimodal distribution with larger pores (bolstering permeability) and smaller pores (molecularly dimensioned, improving selectivity). They are starkly different from poly(trimethylsilyl propyne) (PTMSP) (949 m^2 g^{-1}), characterized by a more loosely packed microstructure containing a significant fraction of wide pores. PTMSP thus offers among the highest permeabilities of known polymers with unparalleled vapor/gas reverse-selectivity but very low gas selectivities.[26] Moreover, the smaller pore presence is heavily skewed towards the ultra-microporous region (<7 Å, shaded) for the triptycene-based polyimide relative to PIM-1 and PTMSP. This tightened and highly interconnected microstructure is the basis for the diffusion-dominated transport in KAUST-PI-1 and its ability to unite high permeabilities with high selectivities for significant commercial separations like H_2/N_2, H_2/CH_4 and O_2/N_2.

This communication demonstrates the significant role of the contortion site in controlling the microstructure and gas transport properties of PIM materials, highlighting 9,10-diisopropyltriptycene as a promising moiety for further study. In accordance with the PIM motif, it imparts greater intramolecular flexibility than the traditional spiro center, and the interstitial spaces created by its three-dimensional architecture increase ultra-microporosity key to many applications. It is thus a promising moiety for investigation in various structural contexts, and here it demonstrates one route towards uniting high permeabilities with high selectivities for more commercially viable PIMs in membrane-based gas separations.

Experimental Section

Typical Synthesis of a KAUST-PI: To a dry 25 mL reaction tube equipped with a Dean-Stark trap, nitrogen inlet and outlet, and reflux condenser were added 2,3,5,6-tetramethyl-1,4-phenylene diamine (1.0 mmol) and freshly distilled *m*-cresol (7 mL). After stirring at room temperature for 5 minutes, an equimolar amount of dianhydride (1.0 mmol), and isoquinoline (0.1 mL) were added. The reaction mixture was stirred at room temperature for 1 h and the temperature was raised gradually to 200 °C and kept at that temperature for 4 h under steady flow of nitrogen. During this period water formed by the imidization reaction was removed by azeotropic distillation using anhydrous toluene. The fibrous polyimide was obtained by the dropwise addition of the polymer solution to an excess of methanol (300 mL). The resulting solid was filtered and dried in an oven at 110 °C. Purification was achieved by reprecipitation from chloroform into a 2:1 methanol/tetrahydrofuran mixture and dried at 120 °C in a vacuum oven for 20 h to give KAUST-PI-1 as an off-white powder in 97% yield. ^{1}H-NMR (400 MHz, $CDCl_3$, δ): 1.82–2.18 (br m, 24H), 3.3–3.6 (br m, 2H), 7.1–7.9 (br m, 12H). FT-IR (Film) $\nu = 1778$ (asym C = O, str), 1720 (sym C = O, str), 1356 (C-N, str), 746 (imide ring deformation) cm^{-1}. GPC ($CHCl_3$): $M_n = 80\,000$ g mol^{-1}, $M_w = 158\,000$ g mol^{-1} relative to polystyrene, $M_w/M_n = 1.98$. BET surface area = 752 m^2 g^{-1}, total pore volume = 0.531 cm^3 g^{-1} at (p/p_o = 0.98, adsorption). TGA analysis: (nitrogen), thermal degradation commences at T_d ~ 400 °C. Elem. anal. calcd (%) for ($C_{52}H_{38}N_2O_8$) (repeat unit): C, 76.27; H, 4.68; N, 3.42. Found: C, 73.61; H, 4.55; N, 3.21.

Modeling and Gas Transport: Modeling of the dihedral angle distributions was done in Materials Studio (6.0, Accelrys) using energy-minimized conformers (Forcite and Conformer modules). Isotropic polymer films were obtained by slow evaporation of a filtered, 3–5 wt% chloroform solution at room temperature from a leveled glass plate. Dry membranes were soaked in methanol for 24 hours, air-dried, and then heated at 120 °C for 24 hours under high vacuum to remove any traces of residual solvent. The pure-gas permeabilities of the membranes were determined at 35 °C and 2 bar using a constant-volume/variable-pressure apparatus. After sufficient degassing, the permeability coefficient, P, was determined from the slope in the steady-state region of the downstream pressure-rise curve. The average diffusion coefficient, D, was calculated from the time lag, θ, by $D = l^2/6\theta$, where l is the membrane thickness. Steady-state permeation data were taken after at least 10 time lags.

Supporting Information

Supporting Information is available from the Wiley Online Library or from the author.

Acknowledgments

This research was supported by King Abdullah University of Science and Technology baseline funding for Ingo Pinnau.

Received: December 20, 2013
Revised: January 31, 2014
Published online: March 11, 2014

[1] T. M. Swager, *Accounts Chem. Res.* **2008**, *41*, 1181.
[2] N. T. Tsui, A. J. Paraskos, L. Torun, T. M. Swager, E. L. Thomas, *Macromolecules* **2006**, *39*, 3350.
[3] a) N. B. McKeown, *ISRN Mater. Sci.*, **2012**, *2012*, 16; b) P. M. Budd, B. S. Ghanem, S. Makhseed, N. B. McKeown, K. J. Msayib, C. E. Tattershall, *Chem. Commun.* **2004**, 2, 230.
[4] a) N. B. McKeown, B. Ghanem, K. J. Msayib, P. M. Budd, C. E. Tattershall, K. Mahmood, S. Tan, D. Book, H. W. Langmi, A. Walton, *Angew. Chem.* **2006**, *118*, 1836; *Angew. Chem. Int. Ed.* **2006**, *45*, 1804; b) N. B. McKeown, P. M. Budd, D. Book, *Macromol. Rapid Comm.* **2007**, *28*, 995.
[5] L. M. Robeson, *J. Membr. Sci.* **2008**, *320*, 390.
[6] P. M. Budd, K. J. Msayib, C. E. Tattershall, B. S. Ghanem, K. J. Reynolds, N. B. McKeown, D. Fritsch, *J. Membr. Sci.* **2005**, *251*, 263.
[7] M. Heuchel, D. Fritsch, P. M. Budd, N. B. McKeown, D. Hofmann, *J. Membr. Sci.* **2008**, *318*, 84.
[8] M. Carta, R. Malpass-Evans, M. Croad, Y. Rogan, J. C. Jansen, P. Bernardo, F. Bazzarelli, N. B. McKeown, *Science* **2013**, *339*, 303.
[9] M. Ghosh, K. L. Mittal, Polyimides: fundamentals and applications, Marcel Dekker, New York USA **1996**.
[10] B. S. Ghanem, N. B. McKeown, P. M. Budd, N. M. Al-Harbi, D. Fritsch, K. Heinrich, L. Starannikova, A. Tokarev, Y. Yampolskii, *Macromolecules* **2009**, *42*, 7881.
[11] a) B. S. Ghanem, N. B. McKeown, P. M. Budd, J. D. Selbie, D. Fritsch, *Adv. Mater.* **2008**, *20*, 2766; b) J. Weber, O. Su, M. Antonietti, A. Thomas, *Macromol. Rapid Comm.* **2007**, *28*, 1871.
[12] C. Zhang, Y. Liu, B. Y. Li, B. Tan, C. F. Chen, H. B. Xu, X. L. Yang, *ACS Macro Lett.* **2012**, *1*, 190.
[13] B. S. Ghanem, M. Hashem, K. D. M. Harris, K. J. Msayib, M. C. Xu, P. M. Budd, N. Chaukura, D. Book, S. Tedds, A. Walton, N. B. McKeown, *Macromolecules* **2010**, *43*, 5287.
[14] Y. J. Cho, H. B. Park, *Macromol. Rapid Comm.* **2011**, *32*, 579.
[15] S. A. Sydlik, Z. H. Chen, T. M. Swager, *Macromolecules* **2011**, *44*, 976.
[16] H. C. Mao, S. Zhang, *Polymer* **2014**, *55*, 102.
[17] E. Hoffmeister, J. E. Kropp, T. L. Mcdowell, R. H. Michel, W. L. Rippie, *J. Polym. Sci., Part A-1: Polymer Chemistry* **1969**, *7*, 55.
[18] I. Pinnau, Z. He, A. Morisato, *J. Membr. Sci.* **2004**, *241*, 363.
[19] R. W. Baker, *Ind. Eng. Chem. Res.* **2002**, *41*, 1393.
[20] Q. S. Zong, C. F. Chen, *Org. Lett.* **2006**, *8*, 211.
[21] C. G. Bezzu, M. Carta, A. Tonkins, J. C. Jansen, P. Bernardo, F. Bazzarelli, N. B. McKeown, *Adv. Mater.* **2012**, *24*, 5930.
[22] P. M. Budd, N. B. McKeown, B. S. Ghanem, K. J. Msayib, D. Fritsch, L. Starannikova, N. Belov, O. Sanfirova, Y. Yampolskii, V. Shantarovich, *J. Membr. Sci.* **2008**, *325*, 851.
[23] B. D. Bhide, S. A. Stern, *J. Membr. Sci.* **1991**, *62*, 37.
[24] Y. Yampolskii, I. Pinnau, B. D. Freeman, Materials Science of Membranes for Gas and Vapor Separation, Wiley, Hoboken, NJ USA **2006**.
[25] N. Ritter, I. Senkovska, S. Kaskel, J. Weber, *Macromolecules* **2011**, *44*, 2025.
[26] a) T. Masuda, E. Isobe, T. Higashimura, K. Takada, *J. Am. Chem. Soc.* **1983**, *105*, 7473; b) I. Pinnau, L. G. Toy, *J. Membr. Sci.* **1996**, *116*, 199.
[27] Y. Rogan, L. Starannikova, V. Ryzhikh, Y. Yampolskii, P. Bernardo, F. Bazzarelli, J. C. Jansen, N. B. McKeown, *Polym. Chem.* **2013**, *4*, 3813.